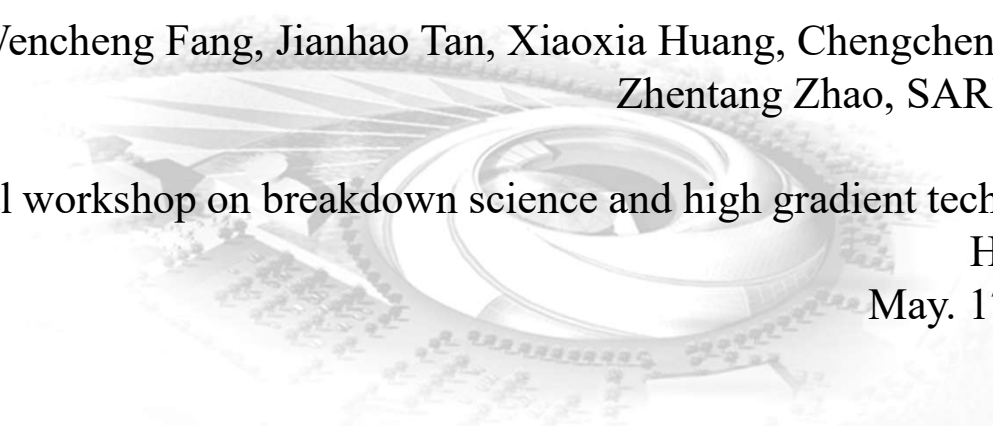


Development of the C-band photocathode gun in SSRF/SARI

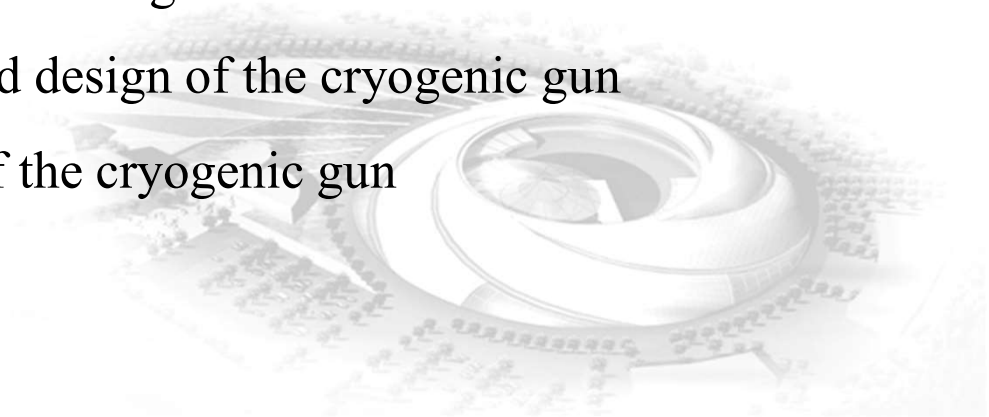
Cheng Wang, Wencheng Fang, Jianhao Tan, Xiaoxia Huang, Chengcheng Xiao,
Zhentang Zhao, SARI/SSRF

International workshop on breakdown science and high gradient technology
HG2022
May. 17, 2022



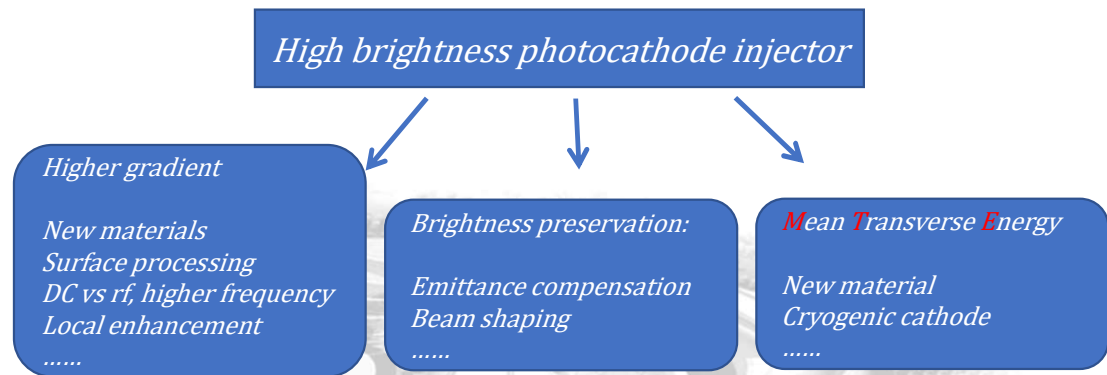
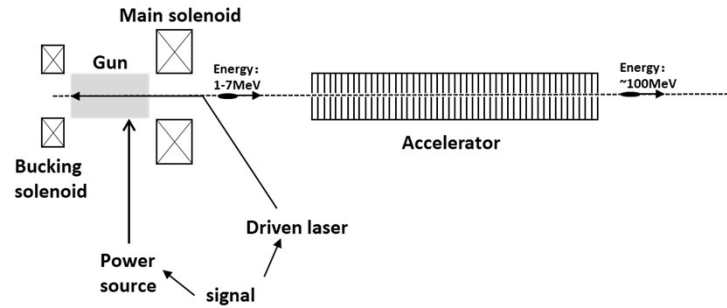
Outlines

- Considerations of Photoinjectors
- The 3.6-cell C-band photocathode gun
 - RF design and features of the gun
 - Experimental results
- The cryogenic photocathode gun
 - Considerations and design of the cryogenic gun
 - Low-power test of the cryogenic gun



Brief introduction

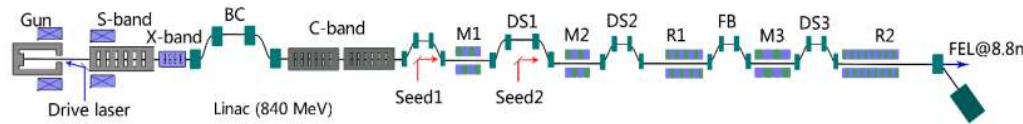
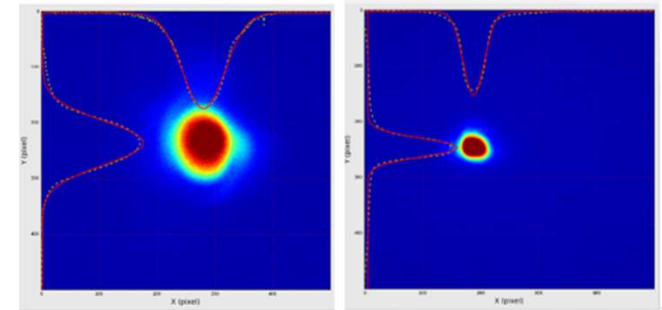
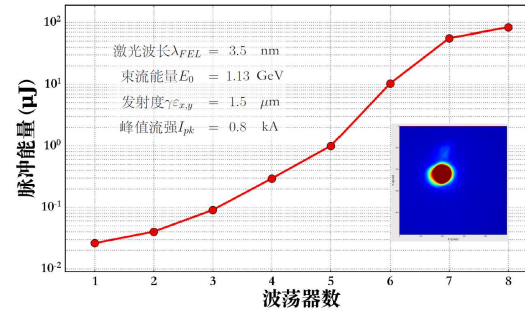
- 1980s
1-2 photocathode gun projects
- 2000s
mature photocathode gun design
- 2020s
Novel gun proposal



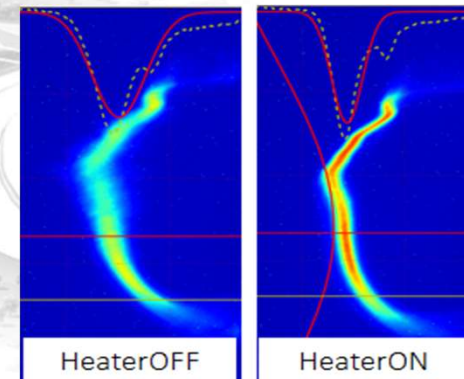
$$\frac{\epsilon_{nCathode}}{\epsilon_{sc}} = \frac{\sqrt{\Delta E_C}}{3mc^2} \frac{1}{\pi 2mc^2} \frac{I_p}{\sin\phi_0 I_A} \mu(A)$$

Brief introduction

- SXFEL has lasing at 5.6nm and 2nm

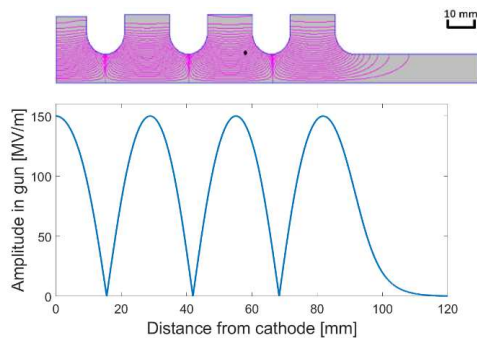
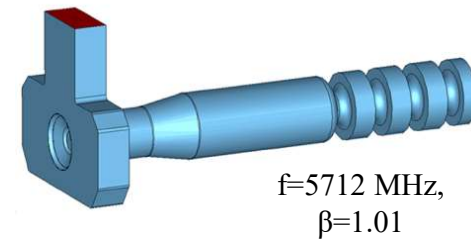


- S-band gun
- 500pC, 10ps electron beam from the gun was compressed below 1ps by chicanes
- Micro-structure caused by the long laser profile shaped by the stacking technique
- Shorter initial beam
- Maintaining the current low emittance

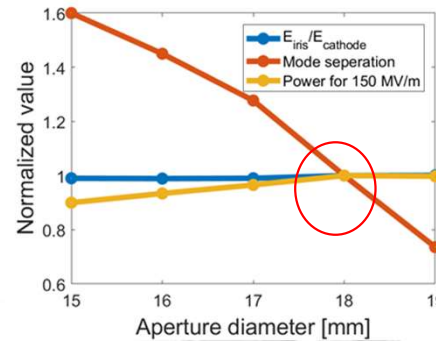


3.6-cell C-band Photocathode RF gun

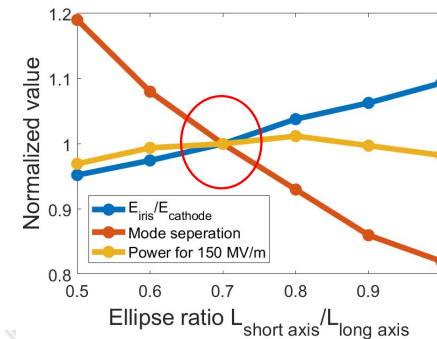
- RF design
- Optimization
 - Mode separation
 - Electric field on the axis and surface
 - Pulsed heat



RF electric field maximum flatness is better than 99%



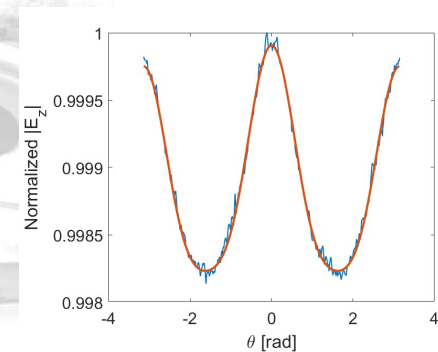
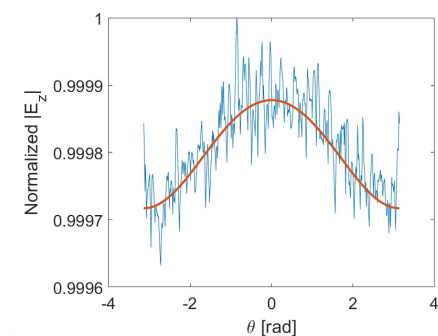
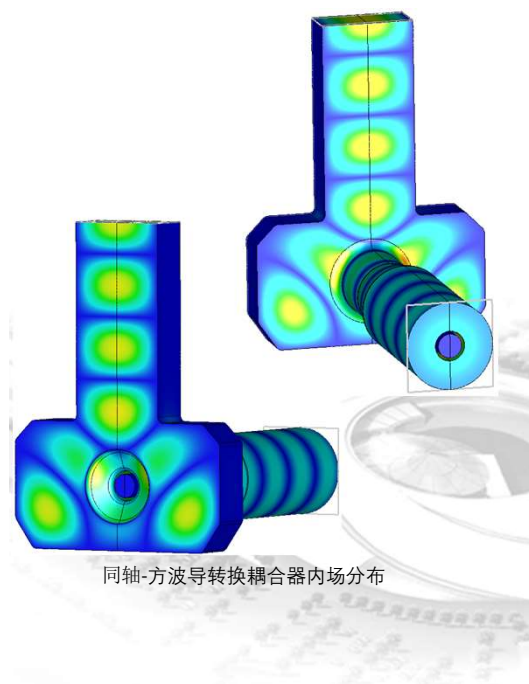
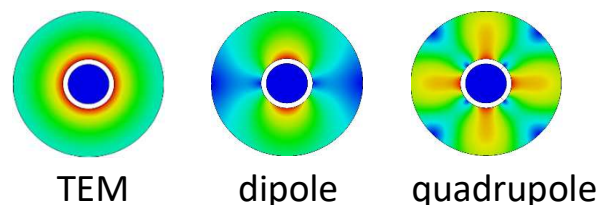
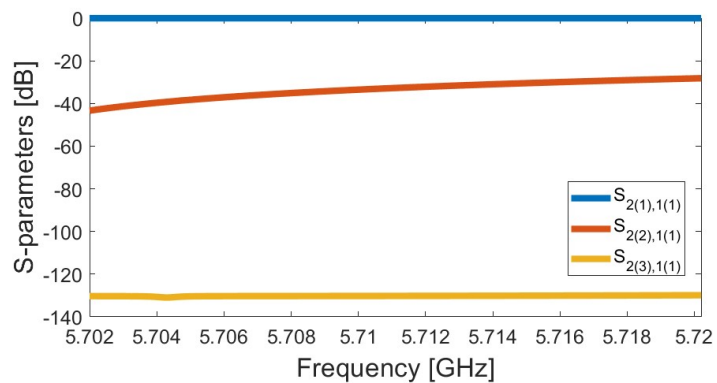
The mode separation varies widely with the aperture diameter, and the peak E varies widely with $L_{\text{short}}/L_{\text{long}}$.



The aperture is 18 mm, and the ratio of the short axis to the long axis of the ellipse is 0.7

RF design

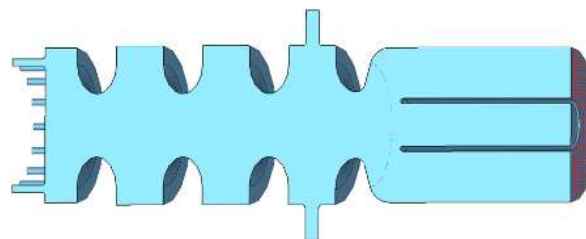
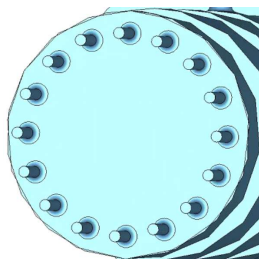
- RF coupler
 - Rectangular waveguide – coaxial cable
 - Eliminate asymmetries
 - Optimized single-feed coupler
 - Dipole-mode is eliminated (almost -40dB)
 - S-parameters of the coupler
 - $S_{2(2),1(1)}$ is the dipole mode
 - $S_{2(3),1(1)}$ is the quadrupole mode



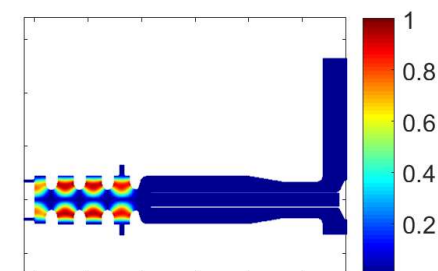
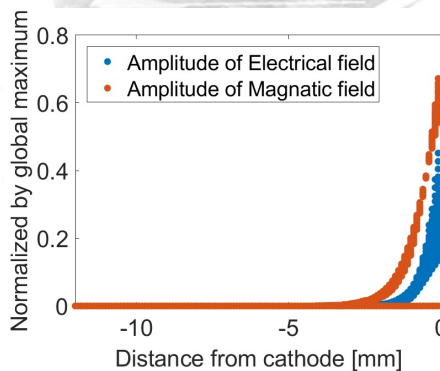
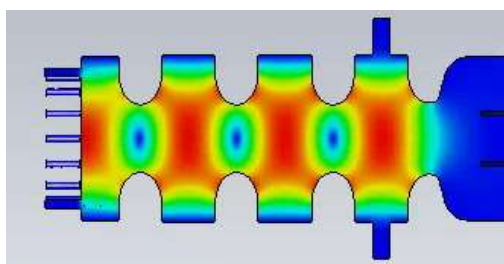
With pick-up port

RF design

- Additional vacuum port on cathode plate.
 - The vacuum ion pump is far away from the cathode
 - Maintaining the quantum efficiency of the cathode
 - Extending photocathode life

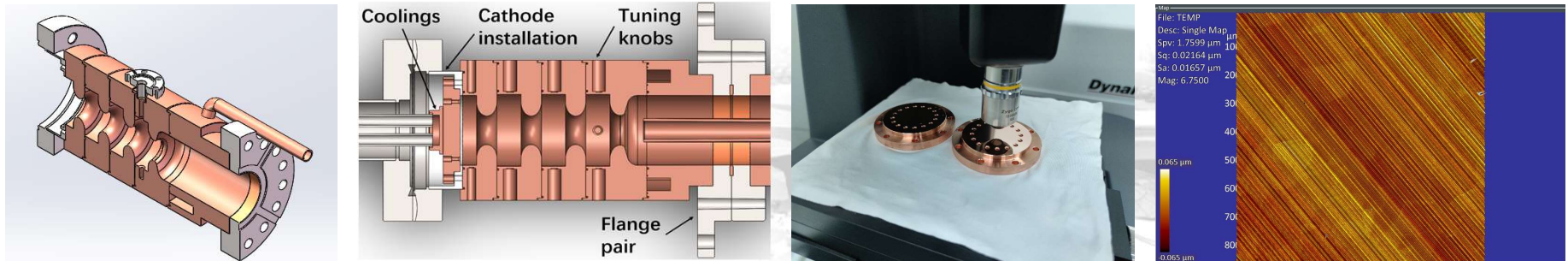


- The additional holes are away from the high field area
 - Rapid decay
 - Will not lead to a significant increase in the chance of breakdown



RF design

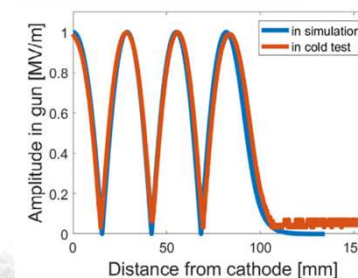
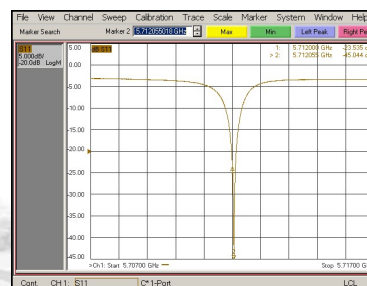
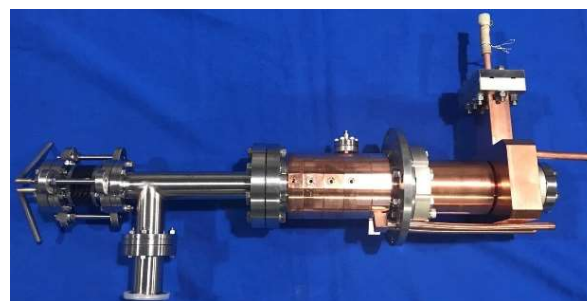
- Removable cathode
 - Mount on the gun cavity (instead of brazing)
 - External cooling head outside
 - The surface roughness of the non-cathode parts is $0.2 \mu\text{m}$.
 - Off-center machining with lathe: RMS roughness $\rightarrow 0.022 \mu\text{m}$.
 - Dry ice cleaning: Removes contaminants such as particles and dirt while maintaining dry



RF design

- RF performance of the C-band gun

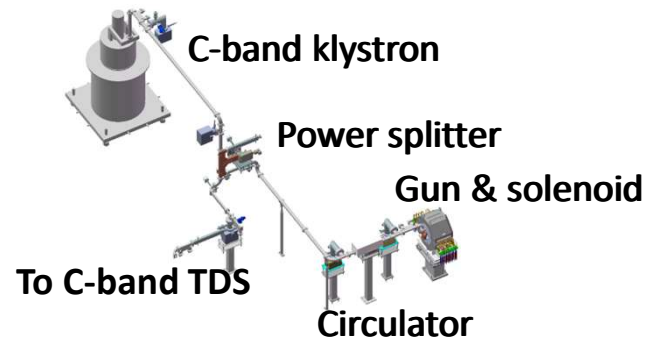
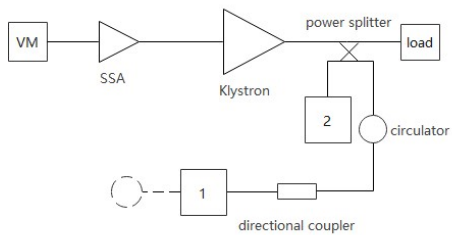
Frequency (π mode)	5712	MHz
Frequency ($2\pi/3$ mode)	5693.61	MHz
Q0	10884	
E _{max} /E _c	0.94	
Shunt impedance	7.414	Mohm
Adjacent mode (cathode)	0.02	
Adjacent mode (cell 1)	0.01	
Adjacent mode (cell 2)	0.005	
Adjacent mode (cell 3)	0.01	
Design gradient	150	MV/m
Peak RF power	14	MW
RF pulse	2.5	μ s
Max(Sc)	2.7	$W/\mu m^2$



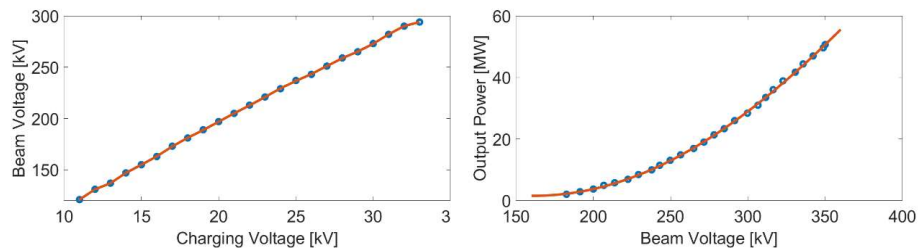
Parameter	Unit	Simulation	Measurement
Frequency	MHz	5712.0	5712.4
Adjacent mode	MHz	18.0	18.0
Q	1	10141	8709

Experimental result

- Vacuum environment and correct temperature
- High power experiment set-up

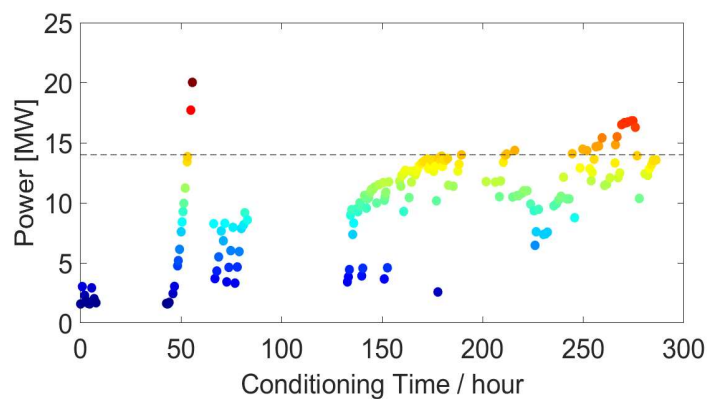
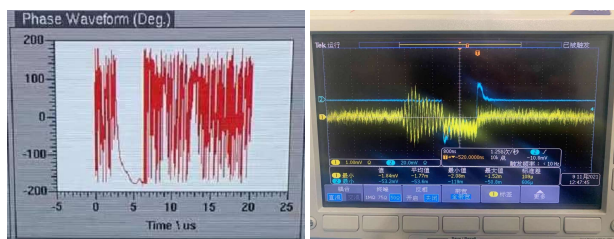
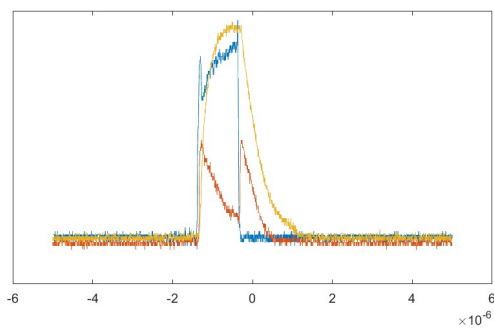


- 50MW C-band klystron;
- LLRF is for C-band based on SXFEL;



Experimental result

- Repetition rate is 10Hz, and from 0.5 μ s to 2.5 μ s
- The gradient in the gun can be figured out from the klystron output
 - 28kV \rightarrow 14 MW \rightarrow 150 MV/m
 - 31kV \rightarrow 20 MW \rightarrow 180 MV/m
 - The gradient reached the goal successfully, and the maximum achievable gradient is 180MV/m



Max E field on the gun[MV/m]	130	140	150	160
Beam energy[MeV]	6.3	6.8	7.3	7.8
Emittance of the injector [mm·mrad]	0.63	0.47	0.44	0.43

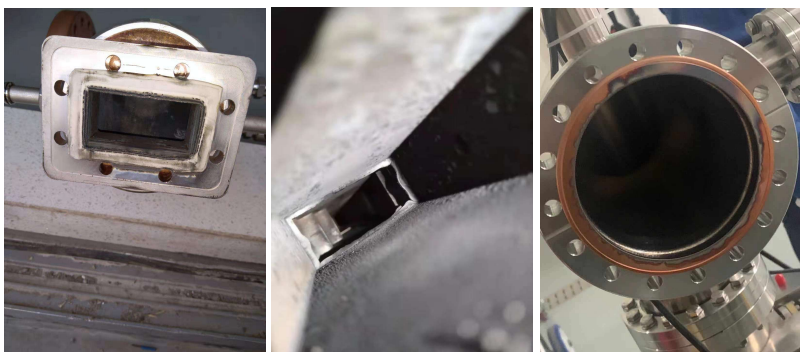
500pC, 5ps

Experimental result

- Lessons learned

2020.12-2021.1

First test, Charring of the rubber gasket at the pumping waveguide



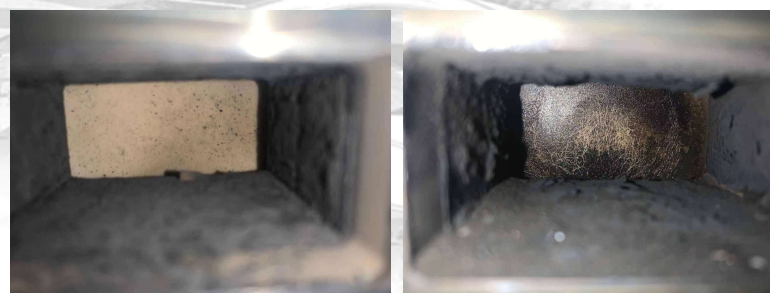
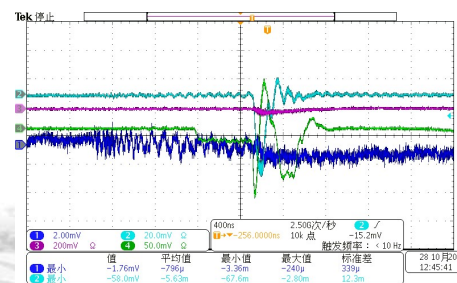
Gas area was contaminated.

New circulator and RF windows.

All flanges based on vacuum type, instead of flat flange.

2021.9-2021.11

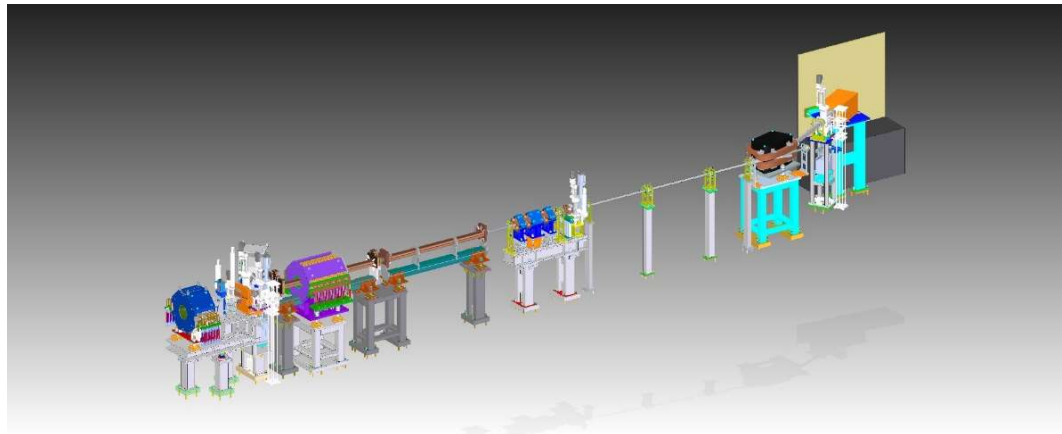
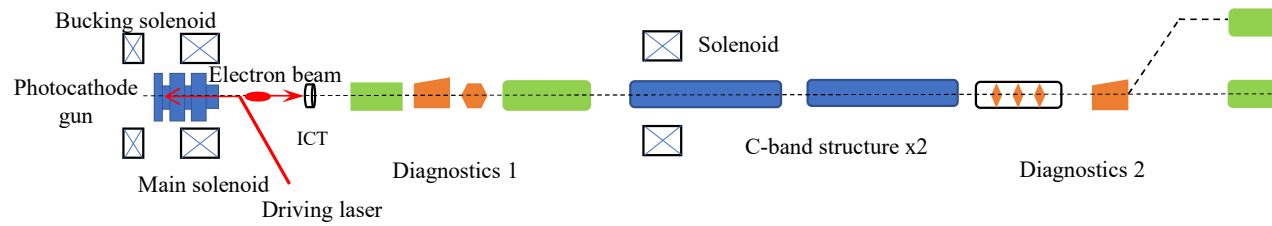
Test again, Breakdown of the circulator



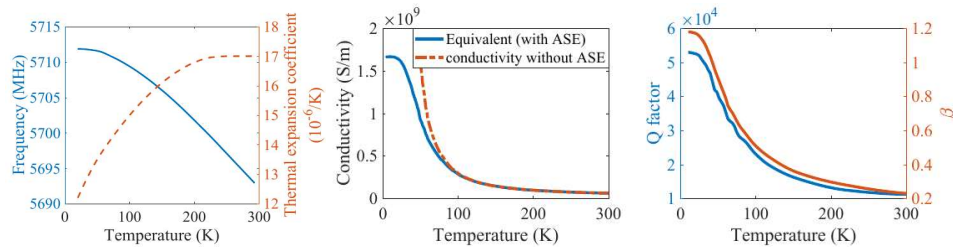
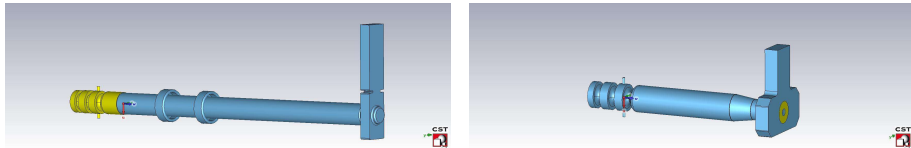
Circulator, above 10MW

Prospect

- Beam testing of the 3.6-cell gun



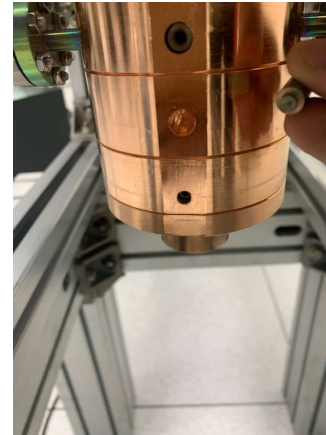
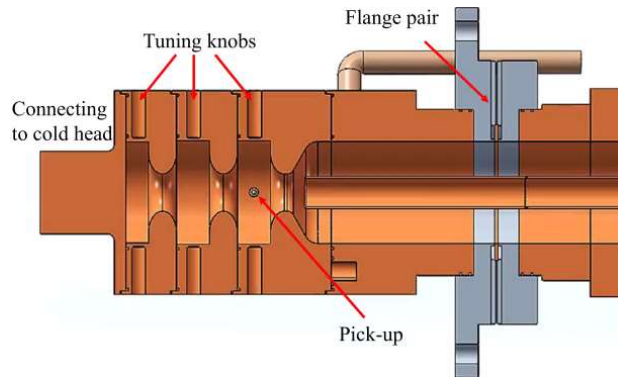
Cryogenic RF gun



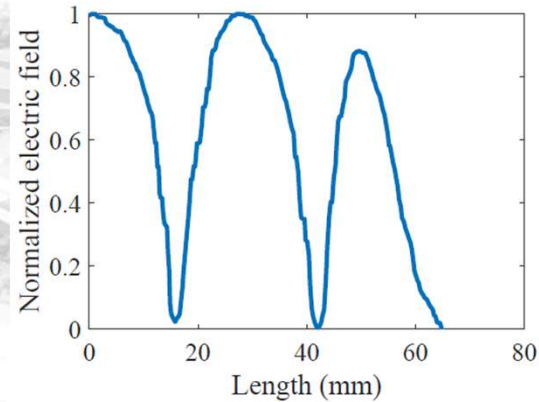
- RRR=500, with ASE in cryo. tem.
- Equivalent conductivity increase by 29
- Q factor, beta, impedance increase by 5.5

	Room temp.	Cryo temp.	
π mode	5692.9	5712	MHz
$1/2\pi$ mode	5674.5	5693.6	MHz
0 mode	5647	5666	MHz
Q0	9852.46	54000	
E _{smax} /E _c	0.914		
Shunt impedance	6.285	34.455	Mohm
Adjacent mode (cathode)	0.0289	0.0094	
Adjacent mode (cell 1)	0.0074	0.0024	
Adjacent mode (cell 2)	0.0226	0.0073	
Target gradient	200		MV/m
Peak RF power	16.773	3.07	MW
RF pulse	2		μ s
Peak temperature rise	75.45	7.8	K

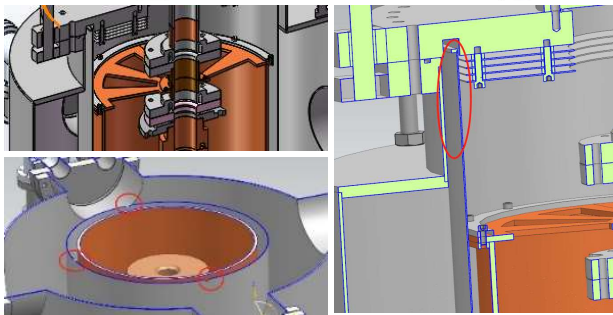
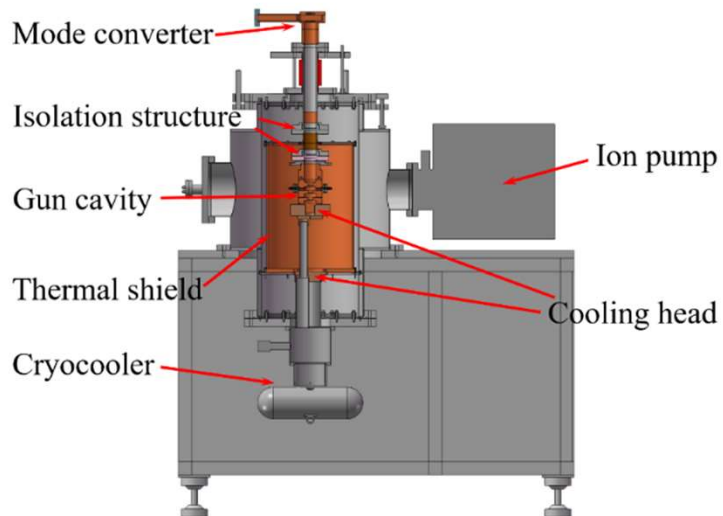
Experimental results of the cryogenic structure



- The prototype cryogenic gun had been fabricated
- Tuning pin disengaged during the low-power test
- Frequency 5695MHz in vacuum, RT
- Field balance 1.12.



Experimental results of the cryogenic structure



Chiller

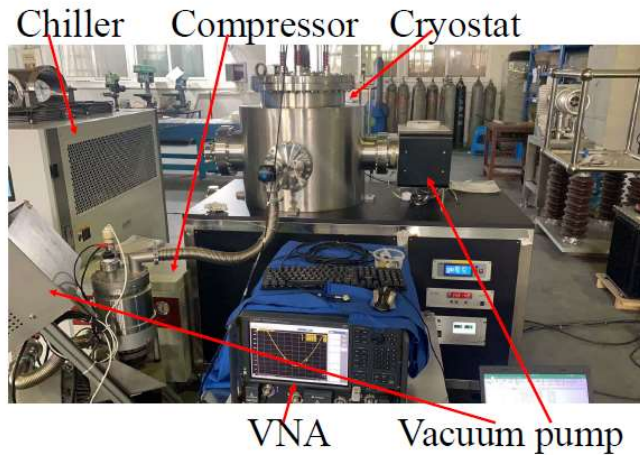
RF structure

**Vacuum
pumping**

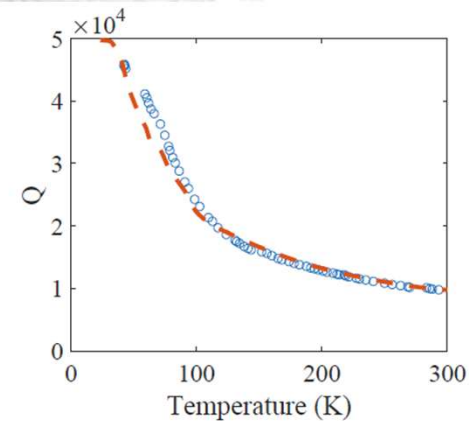
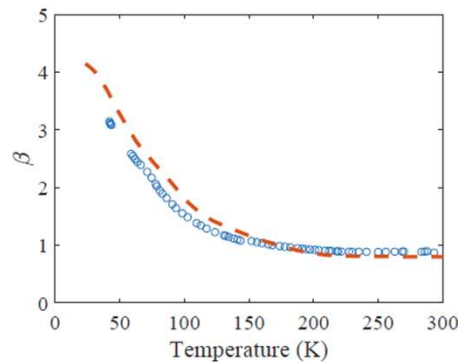
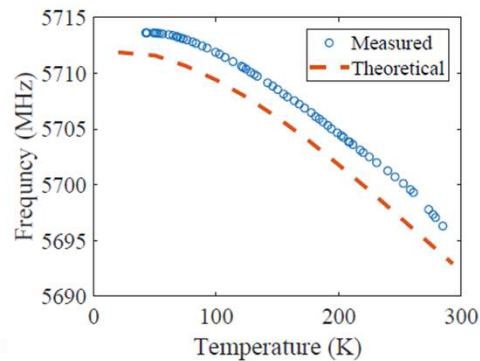


Compressor

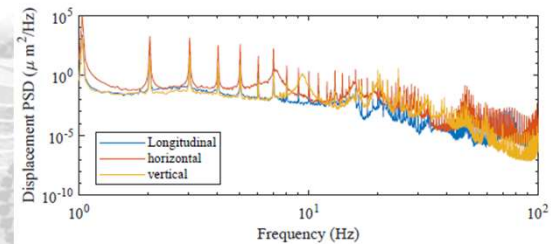
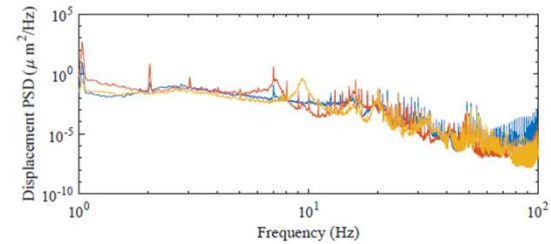
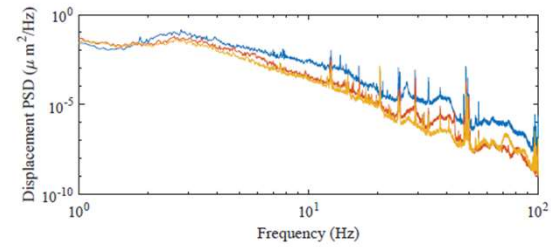
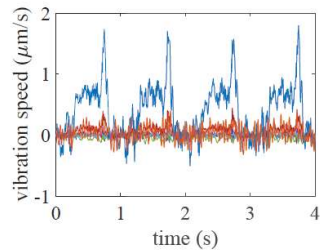
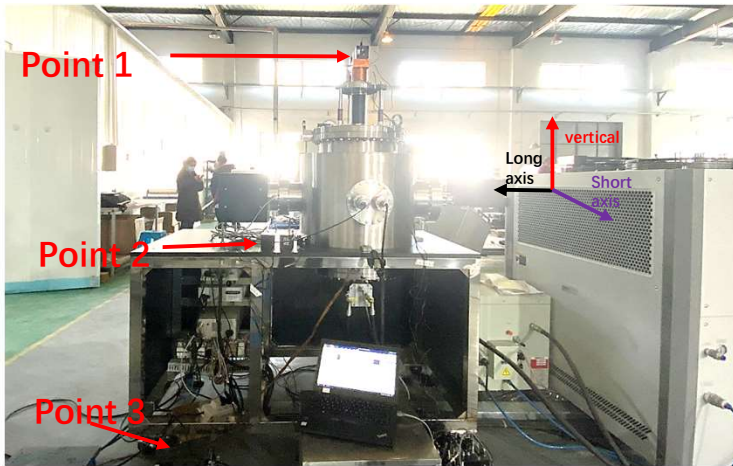
Experimental results of the cryogenic structure



- The cooling time lasted more than 48 h.
- Electron gun reached 40K
- The experimental results are similar with the simulation, with Q factor and coupling about four times higher than at room temperature
- The trend in frequency is consistent with the simulation result, and is currently about 2 MHz off the design frequency due to the electron gun frequency of 5695 MHz



Experimental results of the cryogenic structure



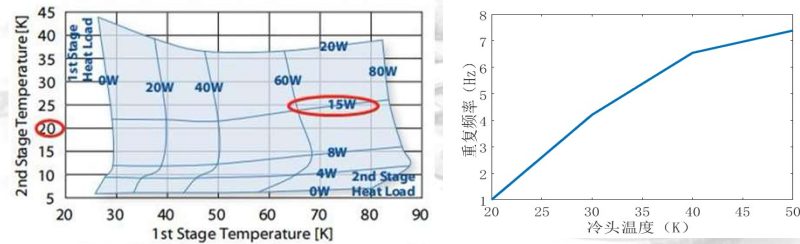
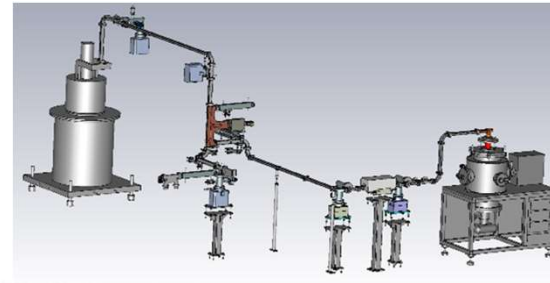
	Vertical	Short axis	Long axis
Point3 (μm)	0.4684	0.3426	0.2901
Point2 (μm)	0.7465	3.9236	0.6129
Point1 (μm)	8.9356	53.1349	7.1549

The vibration mainly occurs within the cross section of the cryo-cooler

The measured vibration amplitude on the cavity is 50 μm

Prospect

- High power study of the cryogenic gun
 - Stability of the operating environment
 - Achievable gradient



Summary

- The development of the C-band electron gun has been largely completed.
- The gun can be operated at 150 MV/m, and can reach the peak gradient of 180MV/m.
- The beam test will be performed at an opportune time.
- The development of the cryogenic gun is underway.

